Nano Research 2016, 9(1): 28–46
DOI 10.1007/s12274-015-0965-x
Review Article
ISSN 1998-0124
CN 11-5974/O4

A mini review on nickel-based electrocatalysts for alkaline hydrogen evolution reaction

Ming Gong[1], Di-Yan Wang[2], Chia-Chun Chen[2,3] (✉), Bing-Joe Hwang[4] (✉), and Hongjie Dai[1] (✉)

[1] *Department of Chemistry, Stanford University, Stanford, CA 94305, USA*
[2] *Department of Chemistry, "National Taiwan Normal University", Taipei 11677, Taiwan, China*
[3] *Institute of Atomic and Molecular Science, "Academia Sinica", Taipei 10617, Taiwan, China*
[4] *Department of Chemical Engineering, "National Taiwan University of Science and Technology", Taipei 10607, Taiwan, China*

Received: 31 October 2015
Revised: 30 November 2015
Accepted: 1 December 2015

KEYWORDS
hydrogen evolution reaction,
nickel,
alkaline electrolyzer,
catalyst

ABSTRACT

High gravimetric energy density, earth-abundance, and environmental friendliness of hydrogen sources have inspired the utilization of hydrogen fuel as a clean alternative to fossil fuels. Hydrogen evolution reaction (HER), a half reaction of water splitting, is crucial to the low-cost production of pure H_2 fuels but necessitates the use of electrocatalysts to expedite reaction kinetics. Owing to the availability of low-cost oxygen evolution reaction (OER) catalysts for the counter electrode in alkaline media and the lack of low-cost OER catalysts in acidic media, researchers have focused on developing HER catalysts in alkaline media with high activity and stability. Nickel is well-known as an HER catalyst and continuous efforts have been undertaken to improve Ni-based catalysts as alkaline electrolyzers. In this review, we summarize earlier studies of HER activity and mechanism on Ni surfaces, along with recent progress in the optimization of the Ni-based catalysts using various modern techniques. Recently developed Ni-based HER catalysts are categorized according to their chemical nature, and the advantages as well as limitations of each category are discussed. Among all Ni-based catalysts, Ni-based alloys and Ni-based hetero-structure exhibit the most promising electrocatalytic activity and stability owing to the fine-tuning of their surface adsorption properties via a synergistic nearby element or domain. Finally, selected applications of the developed Ni-based HER catalysts are highlighted, such as water splitting, the chloralkali process, and microbial electrolysis cell.

1 Introduction

Renewable energy has recently attracted much attention owing to the increasing demand for energy and diminishing fossil fuel resources. Pollution and global warming concerns caused by fossil fuel combustion

Address correspondence to Bing-Joe Hwang, bjh@mail.ntust.edu.tw; Chia-Chun Chen, cjchen@ntnu.edu.tw; Hongjie Dai, hdai@stanford.edu

have also accelerated our need for clean and renewable energy [1–7]. However, the temporal and spatial intermittencies of current renewable energy resources (e.g. solar, wind and geothermal) lead to low energy delivery efficiencies and thereby limit their daily applications [2, 4]. Converting these energy resources into chemical fuels that can be stored and transported is a prospective solution. One of the most promising fuel candidates is hydrogen owing to its high gravimetric energy density, relatively high abundance, and zero emission during consumption [8, 9]. Hydrogen has been produced mainly from an industrial steam reforming process that converts natural gas with water into carbon monoxide and hydrogen, but the low energy efficiency of the conversion process and the presence of carbon-containing residues result in the high cost and low purity of hydrogen products, respectively [10]. An alternative technique of producing hydrogen is via water splitting by electricity or sunlight, which benefits from the abundance of water resources and gives high purity owing to high reaction selectivity [5, 7–9, 11–14].

Hydrogen evolution reaction (HER) is a half reaction of water splitting that reduces protons into hydrogen (reduces water if in alkaline medium) [15, 16]. Even though the reaction involves simple reactants and only two electrons for each hydrogen molecule, the multiple elemental reactions induce an accumulation of energy barriers and result in slow kinetics [15, 16]. A variety of HER catalysts has been found to play significant roles in expediting the reactions. Platinum-based catalysts stand out among all HER catalysts with almost no overpotential at the onset and rapid current increase over voltage increment [14, 15, 17, 18] but are restricted in terms of large-scale utilization by their scarcity and high cost, thus promoting the development of cheap alternatives with high activity and durability. Many non-precious metal-based compounds have been shown to exhibit excellent HER catalytic activity in acid [19–36], but the lack of non-precious counterparts for oxygen evolution catalysis has impeded the development of cost-effective water splitting devices in acidic solutions [12]. The existence of highly active oxygen evolution catalysts that can be used in alkaline condition has spurred the development of novel structures based on non-precious metal for HER catalysis in the alkaline medium [37–46].

Nickel is a first row transition element bearing the atomic number 28. The special properties of nickel metal and compounds enable them to be widely used for various applications, including coins, catalysts, and batteries [47]. Metallic nickel was discovered to catalyze HER in alkaline solutions almost a century ago [48], and researchers have since invested tremendous efforts in understanding the catalytic mechanism and in improving the catalytic activity via electrode design. Recently, more efforts have been undertaken to optimize the chemical structures and morphology of Ni-based heterogeneous catalysts, which offer promising HER catalytic activity for an efficient water splitting process. In this review, we first summarize the historical progression of HER catalytic behavior on nickel surfaces as an introduction to nickel-based HER catalysts in alkaline solutions. Next, we discuss the recent progress associated with nickel-based HER catalysts, including various categories of nickel-based compounds. By understanding the correlation between catalytic activity and chemical composition or catalyst active site, we hope to offer some insights into the past and future of nickel-based HER catalysts. Finally, the applications of these nickel-based catalysts in the water splitting or chloralkali industry are highlighted.

2 HER in alkaline medium

The mechanism of electrocatalytic hydrogen evolution has been extensively studied in the last century. The reaction proceeds via either a Volmer-Tafel or Volmer-Heyrovsky mechanism depending on the catalytic surface [16, 49, 50]. Even though the two general mechanisms can be applied to hydrogen evolution in both acidic and alkaline media, the different pH value leads to different reactants and products in each elemental step owing to the different dominant species that exist in the electrolyte [16, 49, 50]. In alkaline media, the Volmer step is the reduction of a water molecule, adsorbed on the catalyst surface, into an adsorbed hydrogen atom and negatively charged hydroxide anion. Subsequently, the adsorbed hydrogen atom can either be combined with another adsorbed hydrogen atom (formed by the Volmer step) to generate a hydrogen molecule that leaves the surface (the Tafel step), or

attacked by another water molecule to produce a hydrogen molecule and a hydroxide anion (the Heyrovsky step).

$$H_2O + e \rightarrow H_{ads} + OH^- \quad \text{Volmer}$$
$$H_{ads} + H_{ads} \rightarrow H_2 \quad \text{Tafel}$$
$$H_{ads} + H_2O + e \rightarrow H_2 + OH^- \quad \text{Heyrovsky}$$

A significantly lower catalytic activity and exchange current density have been observed on heterogeneous catalysts (e.g. platinum) in alkaline media compared to those in acidic media [49, 50]. This suggests that different reaction pathways can greatly affect the catalytic activity by changing the thermodynamic and kinetic properties. For example, the Volmer step in acid only involves the reduction of a proton into an adsorbed hydrogen atom, therefore suggesting the catalytic activity is strongly correlated to the adsorption energy of the hydrogen atom and researchers have summarized a general "volcano plot" based on this observation [17, 18]. In contrast, the Volmer step in alkaline condition not only depends on the adsorption energy of the hydrogen atom but is also related to the adsorption energy of water and the desorption energy of the hydroxide anion. Low water adsorption energy can lead to insufficient reactants, while high hydroxide anion adsorption energy causes a poisoning effect owing to a loss of catalytically active site. The introduction of additional parameters creates a complicated process of catalytic hydrogen evolution in alkaline medium and this may explain the deviations of transition metals from the "volcano plot" [18]. Therefore, designing heterogeneous HER catalysts with optimal activities in alkaline condition should consider the aforementioned parameters.

3 HER electrocatalysis on Ni metal

The HER mechanism on metallic Ni has been widely studied since the early 1960s. The reactions proceed via pathways identical to the general pathways of alkaline HER, i.e. the Volmer-Tafel or Volmer-Heyrovsky mechanisms [51–53]. Devanathan et al. investigated the HER mechanism on Ni by determining the degree of coverage using the double-charging method [51]. The low coverage values at low cathodic current densities up to 0.5 mA/cm^2 suggested that the rate-determining step is likely the slow discharge of the H_2O molecule or the Volmer step. The gradient of log i_c vs log θ (i_c is the cathodic current density and θ is the coverage value) was determined to be around 2, proving that a rapid Tafel recombination process is the desorption step. Deviations from the Tafel plot at low current densities have been observed and attributed to the reverse reaction that ionizes the H atom or H_2 molecule formed. The larger errors of the coverage values, obtained via the double charging method at high current density due to the re-adsorption of H_2, have limited their claim to the mechanism at low current densities.

A few past studies have proposed the Volmer step as the rate-determining step and the more favorable Volmer-Tafel route for hydrogen evolution, but there have also been reports disputing these early proposals based on data obtained by modern techniques. For instance, Diard et al. claimed that the Volmer-Heyrovsky mechanism is possible owing to the observation of an inductive component in the low frequency range as measured by impedance spectroscopy [54]. Kreysa et al. argued on the possible rate determining step of Tafel recombination due to a slow H_{ads} diffusion [55]. Meanwhile, using steady-state voltammetry and impedance spectroscopy, Krstajic et al. concluded that within a specific potential region, the reaction mechanism follows the Volmer-Tafel route but undergoes the Volmer-Heyrovsky step above a certain potential value; and the rate is possibly controlled by the Heyrovsky step [53]. To date, there is still no common consensus on the alkaline HER mechanism on Ni surfaces.

With regard to the stability of Ni-assisted HER electrocatalysis, researchers have observed a large increase in overpotential over time [56]. Some have ascribed the decay to the formation of nickel hydride, confirmed using X-ray diffraction and scanning electron microscopy [57]. The intrinsically lower HER activity of nickel hydride relative to metallic nickel is attributed to the lower state density of the d-band electrons, which require a higher potential to maintain the same current density. The hydride formation has also been found to change the reaction pathway into a desorption-limited reaction, which might lead to a higher voltage

by increasing the Tafel slope [57]. The hydride could be formed by HER intermediates or a reaction between metallic Ni and dissolved hydrogen in the electrolyte [58]. Some researchers have previously observed the surface oxidation of Ni or electrochemical adsorption of the hydroxide anion in a low overpotential region [59]. The H intermediate formed on the surface could then be replaced by the hydroxide anions to form water and metallic Ni, thus lowering HER activity. These processes might also contribute to the decay of HER activity observed on Ni.

Despite a long history, the mechanisms of HER activity and their stability on metallic Ni surfaces are still being debated, hence necessitating further investigations using modern techniques. Nevertheless, efforts to increase the activity and stability of Ni-based HER catalysts have witnessed significant progress.

4 Recent progress

4.1 Nano-sized Ni metal or Ni-based alloy

The emergence and rapid development of nano-technology has enabled us to build nanostructures with a uniform size and morphological distribution aided by facile synthetic procedures [60–65]. For electrocatalysis, the significantly higher surface area afforded by the nanostructures can dramatically improve the current density at the same overpotential by increasing the accessibility of electrolytes to active surfaces. Ni nanostructures with high surface area can be synthesized using various methods, including bottom-up synthesis via the reduction of nickel salts as well as top-down template-based synthesis [66–69]. Nano-sized Ni powders and porous Ni foams synthesized via bottom-up or top-down methods have been widely used as alkaline battery additives and battery substrates [69, 70]. In addition, Ni nanostructures with various sizes and orientations can be obtained using well-controlled electro-deposition methods on different substrates [71–73].

Ahn et al. synthesized Ni-based dendrites, particles, and films via a controlled electro-deposition procedure using nickel chloride and compared their HER activities based on the different morphologies and against commercial Ni foil (Fig. 1) [73]. The HER activity trend matched the trend of the electrochemical surface areas (ECSA) with dendrite > particle > film > foil. Moreover, McArthur et al. have synthesized size-reduced Ni nanoparticles on top of multi-walled carbon nanotubes via pulse laser ablation (PLA) for hydrogen evolution in alkaline condition, resulting in even higher HER activity [74]. However, owing to their identical chemical nature, these Ni structures exhibit similar electrochemical behavior and their current density scale up almost linearly with increasing surface areas. A Ni structure with the highest surface area can be expected to provide an optimal HER activity but it would still be limited by the intrinsic catalytic activity of metallic Ni. Therefore, to further improve the catalytic activity, researchers have begun tuning the chemical environment of Ni, in addition to taking advantage of the high surface areas of Ni-based nanostructures.

The properties of Ni can be tuned by the introduction of additional elements into metallic Ni to form Ni-based alloys. A nearby hetero-atom has the ability to alter surface adsorption/desorption energy on the adjacent Ni atom, and it may also provide adsorption/desorption sites for certain intermediates to facilitate the catalytic process on Ni. In the 1980s, Brown et al. first investigated a variety of alloys as potential candidates for HER catalysts [75]. Thereafter, Aruraj et al. studied Ni-based binary and ternary alloy co-deposits for the same purpose. The activity trend of Ni-based binary alloys followed Ni-Mo > Ni-Zn > Ni-Co > Ni-W > Ni-Fe > Ni-Cr > Ni-plated steel [76], while the corresponding trend of Ni-Mo-based ternary alloys followed Ni-Mo-Fe > Ni-Mo-Cu > Ni-Mo-Zn > Ni-Mo-Co ~ Ni-Mo-W > Ni-Mo-Cr [77]. Optimized Ni-Mo-Fe electrodes could deliver a current density of 300 mA/cm^2 at an overpotential of 0.187 V and 353 K, for over 1,500 h, with more than 300 mV overpotential advantage over commercial steel plate. Since then, other controlled electrodeposition methods of Ni-based alloys have been developed for HER catalysis [78, 79].

For industrial application, the chemical synthesis of powders that can be pasted onto conductive substrates is still preferred. With the aid of nanotechnology, Ni-based alloy nanostructures have been successfully synthesized with high activity and stability toward HER electrocatalysis [80, 81].

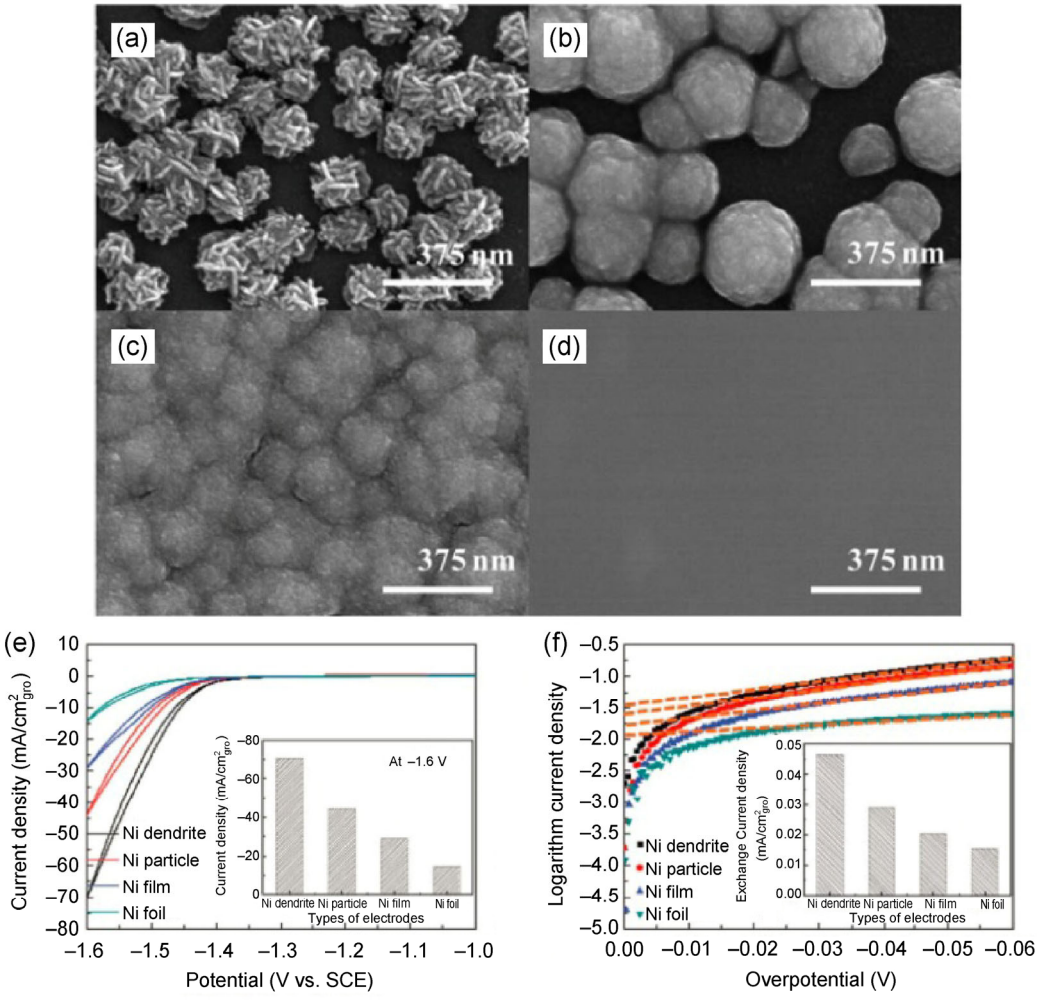

Figure 1 (a)–(d) Field emission scanning electron microscopy (FESEM) images of (a) Ni dendrite, (b) Ni particle, (c) Ni film, and (d) commercial Ni foil. (e) Cyclic voltammetry (CV) curves of various Ni catalysts in 6.0 M KOH under a scan rate of 50 mV/s, with the inset showing the corresponding current densities of different Ni materials at –1.6 V vs. SCE. (f) Tafel plots of the various Ni catalysts, with the inset showing the exchange current densities of different Ni materials. (Reproduced with permission from Ref. [73], © The Royal Society of Chemistry 2012.)

For example, unsupported Ni-Mo alloy nanopowders were prepared by McKone et al. via a slow decomposition of mixed Ni and Mo salts into mixed Ni/Mo oxides or hydroxides, and a subsequent annealing under reducing atmosphere to convert these intermediates into Ni-Mo alloys (Fig. 2(a)) [81]. The powders were then suspended in solvents and cast onto substrates under various loadings for HER activity and stability measurement. The Ni-Mo nanopowder electrodes exhibited excellent activity with a current density of 20 mA/cm^2 at a 70 mV overpotential under a low loading of 1.0 mg/cm^2, and a current density of 130 mA/cm^2 at a 100 mV overpotential under a high loading of 13.4 mg/cm^2 in 2 M KOH (Fig. 2(b)). The electrodes also showed no decay at 20 mA/cm^2 for more than 100 h in alkaline electrolyte (Fig. 2(c)). Notably, pure Ni nanopowders with similar sizes and morphology synthesized using the same procedure but in the absence of Mo salts in the precursors showed drastically lower activity compared to the Ni-Mo nanopowder, which suggests that the chemical property on the catalyst surface is critical to the catalytic activity and might play a more important role than the physical properties (e.g. size and morphology). Nevertheless, the detailed mechanism of improved HER activity achieved via surface alloying with hetero-

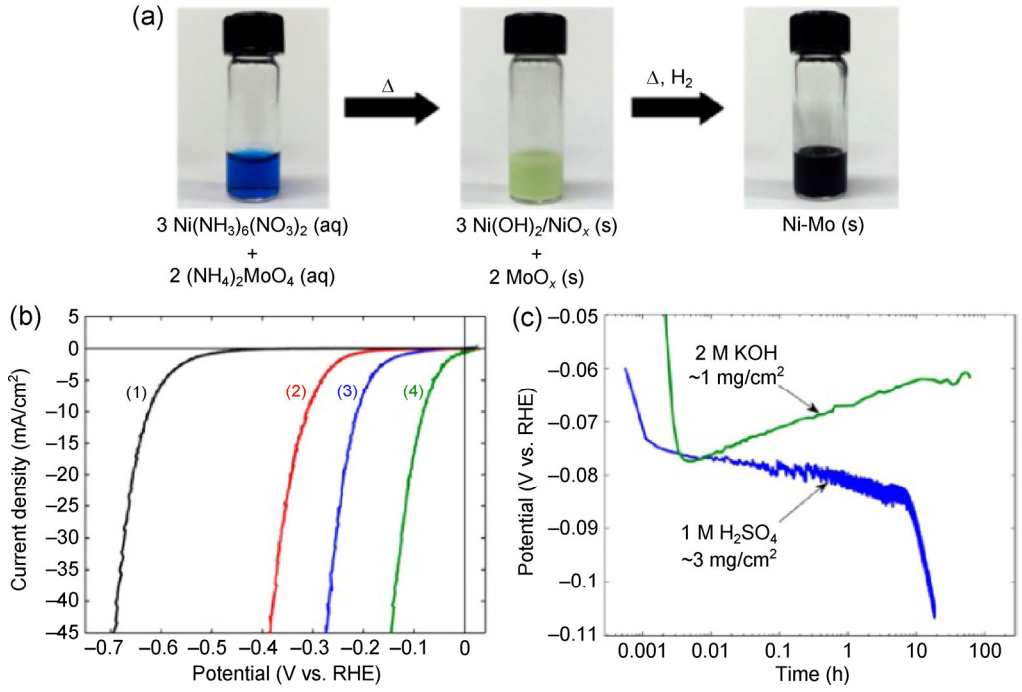

Figure 2 (a) Illustration of synthetic processes with an initial precipitation step, followed by an annealing step under a reducing atmosphere. (b) Comparison of HER catalytic activities of (1) Ti foil substrate; (2) smooth Ni wire; (3) Ni nanopowder without Mo alloying on Ti foil (1 mg/cm^2); (4) Ni-Mo nanopowder on Ti foil (1 mg/cm^2) in 1 M NaOH solution with Ni mesh counter electrode and Hg/HgO (1 M NaOH) reference electrode. (c) Stability curves of Ni-Mo nanopowder on Ti foil (~1 mg/cm^2) in 2 M KOH and (~3 mg/cm^2) in 1 M H_2SO_4. (Reprinted with permission from Ref. [81], © American Chemical Society 2013.)

atoms remains unclear and needs to be studied further. Investigating the oxidation states of Ni and other hetero-atoms on the surface, along with the surface adsorption behaviors of the reactants and intermediates, could help to elucidate the role of surface alloying and facilitate the further optimization of HER catalysts via chemical design.

4.2 Nickel-based oxide/hydroxide

Metallic nickel is normally considered as the most stable phase under HER condition in alkaline solution [82], but the overpotential needed for nucleation of metallic Ni during the reduction of Ni oxide or hydroxide offers the possibility of using Ni-based oxide/hydroxide as a catalyst. Nickel-iron layered double hydroxide (NiFe LDH) is an active oxygen evolution reaction catalyst with superior activity compared to commercial Ir-based catalyst (i.e. a benchmark catalyst) in alkaline solution [12], but Luo et al. have also discovered that NiFe LDH directly grown on Ni foam (NiFe LDH/Ni foam) is highly active for HER catalysis [83]. The NiFe LDH/Ni foam outperformed Ni foam by almost 200 mV at high current densities, and the incorporation of Fe in NiFe LDH produced better catalytic activity compared to pure $Ni(OH)_2$/Ni foam. Although the authors have not elaborated the underlying mechanism, we believe that metallic Ni on the Ni foam remains as the active surface for HER catalysis and NiFe LDH may provide adjacent surface adsorption/desorption sites for the reaction. The synergistic effects of NiFe LDH and Ni foam give rise to the high catalytic activity, and more details will be discussed in the "Nickel-based heterostructure" section.

Bulk Ni oxide or hydroxide is generally considered as HER inactive materials owing to its inappropriate hydrogen atom adsorption energy (excessively strong H adsorption on O, but extremely weak H adsorption on Ni), but the electronic property of the Ni-based oxide can be tuned so as to form suitable surfaces for HER catalysis. Wang et al. have utilized a conversion reaction by lithium ion (Li^+) insertion and extraction,

employed in lithium-ion batteries, to improve the catalytic performance of transition metal oxide [84]. The Li^+ insertion/extraction cycling could greatly reduce the grain size of the transition metal oxide nanoparticles and consequently, increase the catalytic activity; however, excessive cycling leads to amorphous nanostructures with lower activity compared to the one with fewer cycles (Fig. 3(a)). The optimized 2-cycle nickel-iron oxide on carbon fiber paper ($NiFeO_x$/CFP) exhibited excellent activity and stability towards oxygen evolution reaction in 1 M KOH. Interestingly, the 2-cycle $NiFeO_x$/CFP electrode could also significantly reduce the HER overpotential by almost 200 mV in comparison to the pristine $NiFeO_x$/CFP electrode, and only an 88 mV overpotential is required to achieve 10 mA/cm^2 (Fig. 3(b)). The much improved activity is not only a result of the reduced dimension of the nanoparticles, but also might be caused by the fine-tuned electronic property associated with Li^+ insertion/extraction, which could change the oxidation state of the metal cations. The superb HER and oxygen evolution reaction (OER) catalytic activities obtained gave rise to a bifunctional catalyst electrode that is low in cost but highly efficient for water splitting application (Fig. 3(c)).

4.3 Other nickel compounds (sulfide, phosphide, etc.)

A significant progress in the development of transition metal chalcogenide, as well as phosphide materials, to replace precious platinum HER catalysts in PEM electrolyzers has been made recently [19, 20, 22–32, 34–36]. Nickel-based compound is one of the most interesting candidates screened and good catalytic

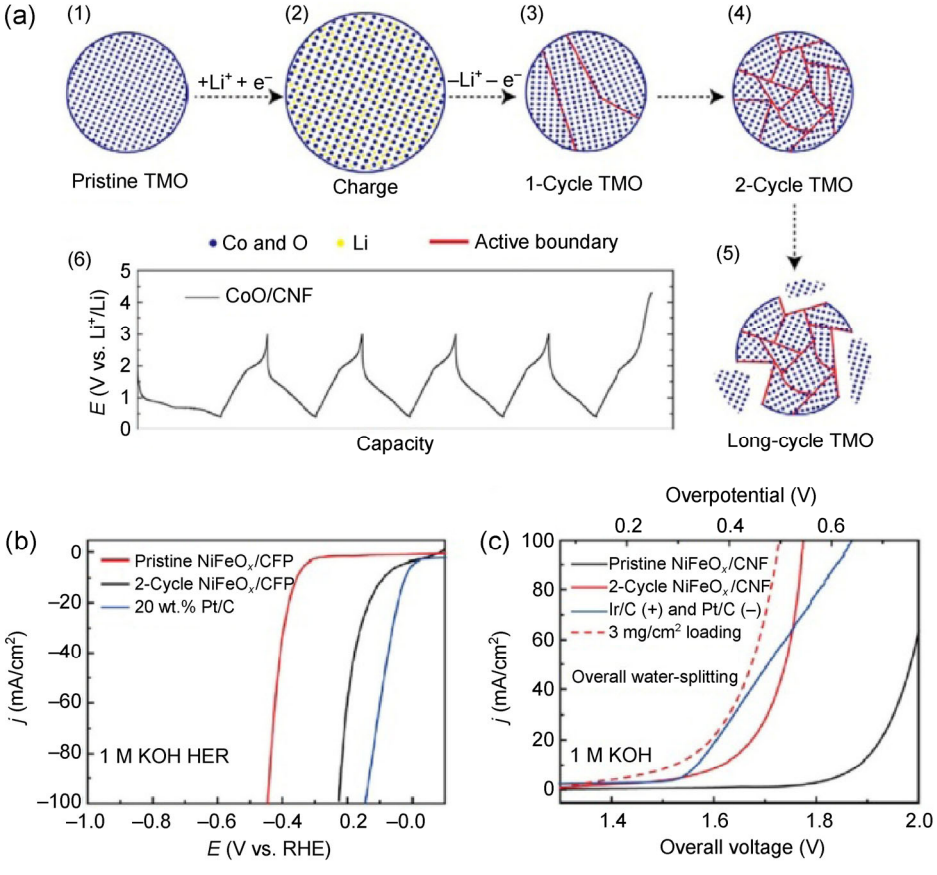

Figure 3 (a) Schematic illustration of transition metal oxide (TMO) morphology evolution under Li insertion/extraction cycles. (b) Linear sweep voltammetry (LSV) curves of 2-cycle $NiFeO_x$/CFP compared to its pristine counterpart and Pt/C benchmark. (c) 2-Cycle $NiFeO_x$/CFP as both HER and OER catalysts in 1 M KOH for water splitting in comparison to Ir/C and Pt/C benchmarks. (Reprinted with permission from Ref. [84], © Nature Publishing Group 2015.)

activity has been observed. Among these nickel-based compounds, nickel molybdenum nitride ($NiMoN_x$) [85] and nickel phosphide (Ni_2P) [25] stood out, showing comparable activity to a Pt-based benchmark catalyst. However, most existing studies focused on HER electrocatalysis in acids and there are fewer reports on HER activity in alkaline medium. Popczun et al. first reported crystalline Ni_2P nanostructures' high intrinsic catalytic activity towards HER and claimed that these nanostructures could also catalyze HER in alkaline condition (with slightly decreased activity) but they rapidly degraded to metallic Ni during stability measurement [25]. Similar instability was also observed in previous studies using Ni-S [86] and Ni-P alloys [87, 88] as HER electrocatalysts, and this was re-confirmed by other groups synthesizing Ni_2P-based materials for HER catalysis [89, 90]. Nevertheless, Ni_2P and other Ni-based compounds still hold great potentials as highly active HER catalysts in acidic or neutral electrolytes.

4.4 Nickel-based heterostructures

Since HER involves multiple adsorption/desorption processes with multiple species in alkaline media, catalysts with single chemical components might be limited in terms of matching the desired adsorption/desorption energies of each species (e.g. H_2O, OH^-, H atom, and H_2). The best Pt catalyst exhibited lower HER activity by two or three orders of magnitude in alkaline conditions [50]. Introducing a second component in an intimate junction with the single-component Ni catalyst to form a hetero-structured interface may create more opportunities in tuning the adsorption/desorption energies, thereby forming more active catalysts.

Subbaraman et al. first established a hetero-junction system by constructing nano-sized $Ni(OH)_2$ clusters on Pt electrode to improve the catalytic activity of Pt in alkaline electrolytes [91]. Even though the incorporation of $Ni(OH)_2$ nano-clusters onto Pt(111) surfaces led to a 35% decrease of exposed Pt(111), as probed by the current-potential curves in the underpotentially deposited hydrogen (H_{upd}) region, the HER activity of the $Ni(OH)_2$/Pt(111) electrode outperformed that of Pt(111) by ~7 times (Fig. 4(a)).

They proposed that H_2O specifically adsorbs on the $Ni(OH)_2$/Pt(111) interface with O atoms interacting with $Ni(OH)_2$ domains and H atoms interacting with Pt surface near the boundary. Subsequently, H_2O dissociates into an adsorbed H atom that moves to vacant Pt sites nearby, as well as a OH^- anion that desorbs from the $Ni(OH)_2$ sites. Finally, two adsorbed H atoms generated from the H_2O dissociation process combine with each other to form H_2 on Pt surfaces, before undergoing desorption (Fig. 4(b)). The improvement in catalytic activity obtained via the incorporation of $Ni(OH)_2$ was applied to other surfaces, such as Pt(110) and nano-Pt, implying that metal oxide/hydroxide-metal interfaces could function as a general system for the optimization of HER activity in alkaline electrolytes. Subsequently, the group constructed $Ni(OH)_2$ nanoclusters on various metal sites and observed an improvement in HER activity over bare metal sites, matching the activities obtained in acidic electrolytes [92]. Specifically, the activity of $Ni(OH)_2$/Ni structures is enhanced by ~4 times compared to $Ni(OH)_2$ free-Ni structures. Moreover, $Ni(OH)_2$ not only facilitates H_2O dissociation on the surface, but also stabilizes the H_2O-surrounded cations (forming a compact double layer on the surface) so that more H_2O molecules can be attracted to the interfaces for further dissociation. By introducing a Li^+ cation that interacts more strongly with H_2O compared to Na^+ and K^+ cations that are generally used in the electrolyte, the activity of $Ni(OH)_2$-decorated/Pt surfaces is further improved by a factor of 2, while using Pt alone has no such effects (Fig. 4(c)) [91].

In optimizing HER catalytic activity in alkaline media, the number of metal oxide/hydroxide-metal interfaces should be maximized, especially for non-precious metal-based catalysts. Along this line, we have successfully created nanoscale nickel oxide-nickel (NiO/Ni) interfaces via the low-pressure decomposition and reduction of nickel hydroxide grown on top of oxidized carbon nanotubes ($Ni(OH)_2$/ox-CNT) upon annealing under an inert atmosphere [93]. Scanning transmission electron microscopy (STEM) and electron energy loss spectroscopy (EELS) mapping revealed ~10 nm nanoparticles with a core–shell-like structure, with Ni and O in the shell and only Ni in the core over a CNT network (Fig. 5(d)). High-resolution STEM

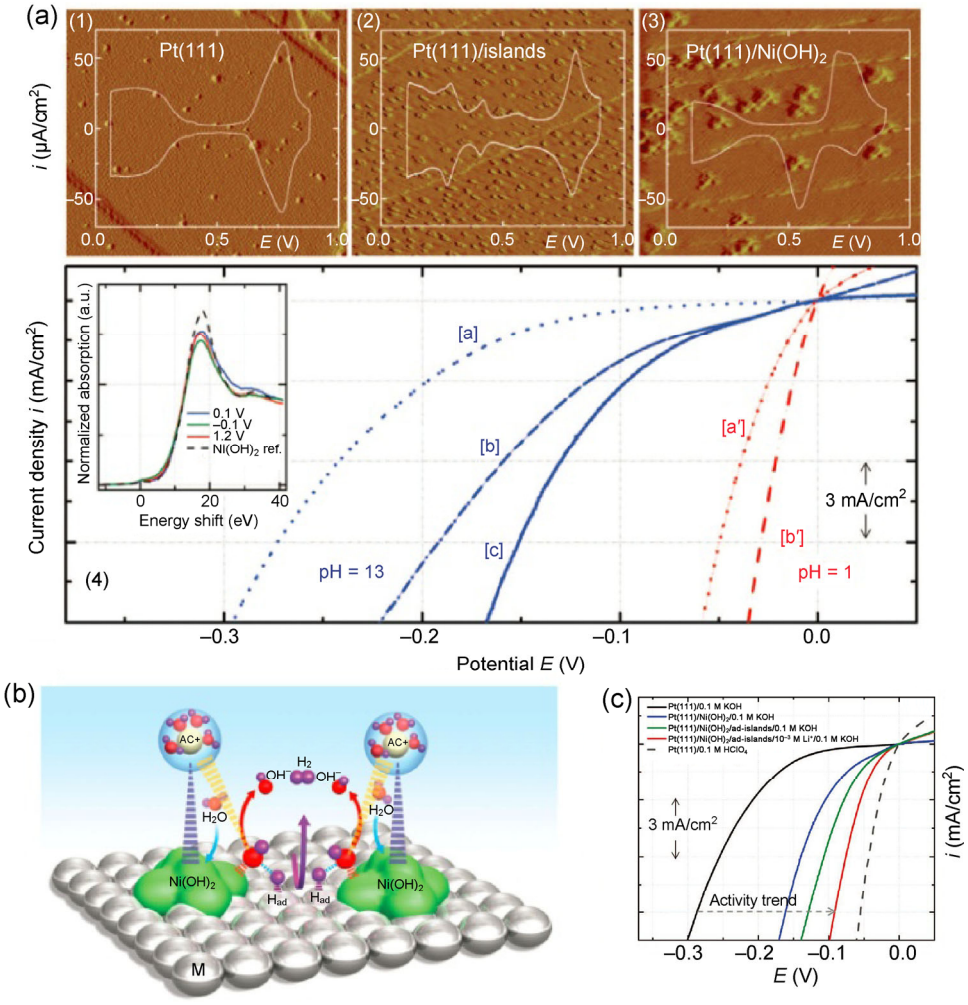

Figure 4 (a) STM images and CV curves for (1) Pt(111), (2) Pt(111) with Pt islands, and (3) Pt(111) modified with $Ni(OH)_2$ clusters in 0.1 M KOH. (4) HER activities for [a] Pt(111); [b] Pt(111) with Pt islands; [c] Pt(111) modified with $Ni(OH)_2$ clusters in alkaline solutions compared to [a'] Pt(111); [b'] Pt(111) with Pt islands in acid solutions. The inset shows $Ni(OH)_2$ XANES spectra under different potentials with a $Ni(OH)_2$ reference spectrum. (b) Schematic illustration of the proposed HER mechanism on Pt(111) modified with $Ni(OH)_2$ clusters in alkaline solutions. (c) Comparison of HER activities with different structures on Pt(111). The red curve shows an improved activity by Li^+ addition for Pt(111) modified with $Ni(OH)_2$ clusters. (Reprinted with permission from Ref. [91], © American Association for the Advancement of Science 2011.)

images showed that the NiO shell contains grains with different orientation and small in-between gaps, exposing many nanoscale NiO–Ni interfaces. The ox-CNT precursors are crucial in delaying the reduction of $Ni(OH)_2$ into large Ni aggregates via Ostwald ripening by spatially separating the individual nanoparticles. By comparing the HER activity with those of pure Ni/CNT and NiO/CNT synthesized by similar methods but at higher temperature and higher pressure respectively, there are significant advantages in having NiO/Ni nano-interfaces that can achieve 10 mA/cm^2 at <100 mV overpotential under a ~0.28 mg/cm^2 loading on glassy carbon, and 100 mA/cm^2 at <100 mV overpotential under an ~8 mg/cm^2 loading in Ni foam (Fig. 5). It is mechanistically proposed that the OH^- anion generated by the Volmer step attaches to the NiO site preferentially at the NiO/Ni interface, and the H atom moves to a nearby Ni site for recombination to generate H_2. Pure NiO surfaces are poor at catalyzing HER owing to its inability to stabilize the H atom, while pure Ni surfaces will eventually be occupied by the OH^- anion generated, thus blocking the active sites.

While the NiO-Ni heterostructure was biased at

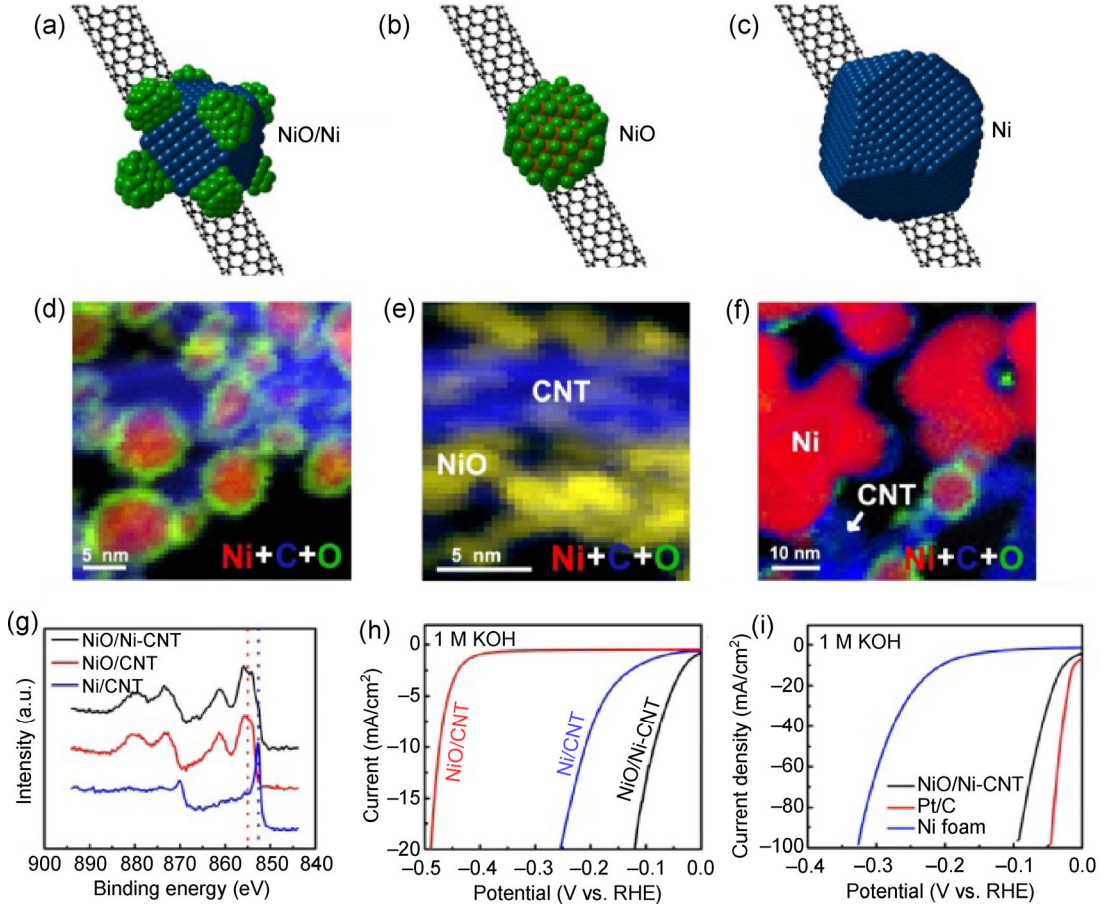

Figure 5 (a)–(c) Schematic illustrations of (a) NiO/Ni-CNT, (b) NiO/CNT, and (c) Ni/CNT. (d)–(f) Reconstructed EELS elemental maps with Ni in red, C in blue, and O in green for (d) NiO/Ni-CNT, (e) NiO/CNT, and (f) Ni/CNT structure. (g) High resolution Ni XPS spectra (the dotted line shows the binding energy of Ni^{2+} (red) and metallic Ni (blue)). (h) LSV curves of catalysts on rotating disk electrodes in 1 M KOH at a scan rate of 1 mV/s (the loading is 0.28 mg/cm^2). (i) LSV curves of catalysts on Ni foam in 1 M KOH at a scan rate of 1 mV/s (the loading of 8 mg/cm^2). (Reprinted with permission from Ref. [93], © Nature Publishing Group 2014.)

constant potential for a long time, we observed an obvious decay in current density, suggesting the instability of the NiO-Ni nanostructures under HER operation conditions (Fig. 6(e)). STEM images and EELS mapping indicated obvious oxidation of the Ni core and some phase separation between NiO and Ni after long-term stability measurement (Figs. 6(a) and 6(b)) [94]. Based on the NiO-Ni hetero-structure, we further introduced a nanoscale Cr_2O_3 phase to form a ternary Ni@NiO-Cr_2O_3 hetero-structure (CrNN) [94]. The HER activity of the CrNN catalyst was comparable to the NiO-Ni hetero-structure owing to the preserved core NiO-Ni active site. More importantly, the CrNN catalyst could achieve long-term HER operation without any decay; and especially at high loadings of 24 mg/cm^2, the electrode could maintain >200 mA/cm^2 for at least 80 h at an overpotential of –250 mV vs. RHE without *iR* compensation (Fig. 6(f)). Even after a long-term stability measurement, the Ni@NiO-Cr_2O_3 ternary structure still remained intact (Figs. 6(c) and 6(d)), implying that Cr_2O_3 is an effective protection layer that holds the core NiO-Ni active site and prevents oxidation by dissolved oxygen or oxygen generated from the counter electrodes.

The use of metal oxide-metal and hydroxide metal interfaces for electrocatalysis is a promising field that provides opportunities for the optimization of electrocatalytic activity by uncovering an appropriate combination of metal oxide/hydroxide and metal. For metallic Ni, which is known to have a suitable H adsorption energy, it is highly likely that a good match (i.e. metal oxide/hydroxide) can be found to

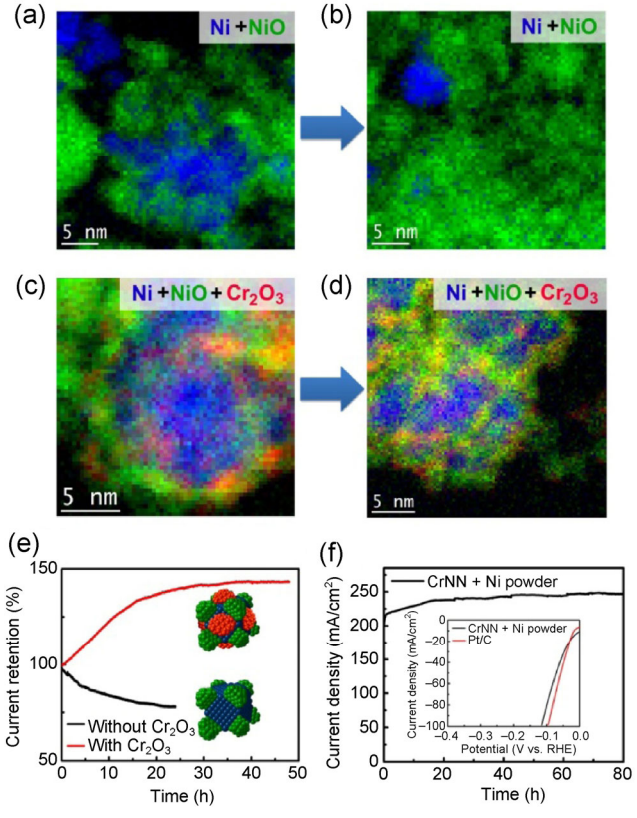

Figure 6 (a) and (b) STEM-EELS chemical maps for Ni (in blue) and NiO (in green) (a) before and (b) after stability, showing oxidation and phase segregation. (c) and (d) STEM-EELS chemical maps for Ni (in blue), NiO (in green), and Cr_2O_3 (in red) (c) before and (d) after stability showing an intact structure. (e) *i*–*t* curves of NiO/Ni heterostructure, with and without Cr_2O_3 with the initial current densities of 20 mA/cm^2. (f) *i*–*t* curves of the CrNN catalyst under a loading of 24 mg/cm^2, with 30 wt.% Ni powder at a constant potential of –0.25 V vs. RHE without *iR* compensation (R = ~0.6 Ω). Inset shows linear sweep voltammetry curves of the CrNN catalyst under a loading of 24 mg/cm^2 compared to 8 mg/cm^2 Pt/C. (Reprinted with permission from Ref. [94], © Wiley-VCH Verlag GmbH & Co. KGaA, Weinheim 2015.)

replace precious metal catalysts by optimizing the adsorption energy of H_2O and OH^-. Such effort requires both theoretical calculations to predict the probable candidates, as well as synthetic methodology to create and maximize the active metal oxide/hydroxide-metal sites.

5 Applications

The half reaction of HER has been widely used for various applications. Splitting water into H_2 and O_2 to obtain H_2 fuels from H_2O sources is the major target for most studies, and is one of the most promising ways of converting renewable energy into transportable chemical fuels. Electrocatalytic water splitting is realized by pairing up HER and OER catalysts in either acidic or alkaline solutions. In acidic solutions, the advantage lies with the availability of proton exchange membranes that conduct protons but not electrons, and these membranes also separate the gases formed to prevent cross-over reactions that decrease the reaction efficiency. However, a major disadvantage is the high cost of precious metal catalysts needed for H_2 and O_2 generation [14]. In comparison, with advances in the development of various HER and OER electrocatalysts possessing high activity and stability (especially Ni-based catalysts), along with a progress in building better anion exchange membranes, the use of alkaline electrolyzers for H_2 production has been actively pursued. Many studies have previously reported superior electrolytic activity and stability in alkaline electrolytes. In our work, we have paired NiFe LDH on Ni foam (as the OER electrocatalyst) and CrNN or NiO/Ni-CNT on Ni foam (as HER electrocatalysts) together in a 1 M KOH electrolyte solution [93, 94]. The electrolyzer afforded a water splitting onset potential of <1.5 V with rapid current increase to 100 mA/cm^2 with a voltage of <1.7 V without *iR* compensation at room temperature (Figs. 7(a) and 7(c)). For an electrolyzer with a CrNN catalyst, it could achieve a current density of 200 mA/cm^2 at ~1.75 V without *iR* compensation, with ~70.2% efficiency (~1.57 V/~78.3% efficiency with *iR* compensation). Our electrolyzer outperformed the industrial alkaline electrolyzer using Ni and stainless steel foils by 510 mV at room temperature, and 370 mV at 60 °C, corresponding to a saving of ~22.8% (in voltage) or ~18.4% (in energy). Electrolysis with the NiO/Ni-CNT catalyst showed a decay of ~20 mV over 24 h under a constant current density of 20 mA/cm^2 (Fig. 7(b)) [93]; and with the incorporation of Cr_2O_3, the stability of the electrolyzer greatly improved, showing no decay over 500 h to achieve 20 mA/cm^2 with <1.5 V of operation voltage (Fig. 7(d)) [94]. Further integration with an efficient GaAs solar cell resulted in a stable H_2 production by solar power, with a high efficiency of ~15% (Figs. 7(e) and 7(f)).

The high activity of Ni-based catalysts for alkaline

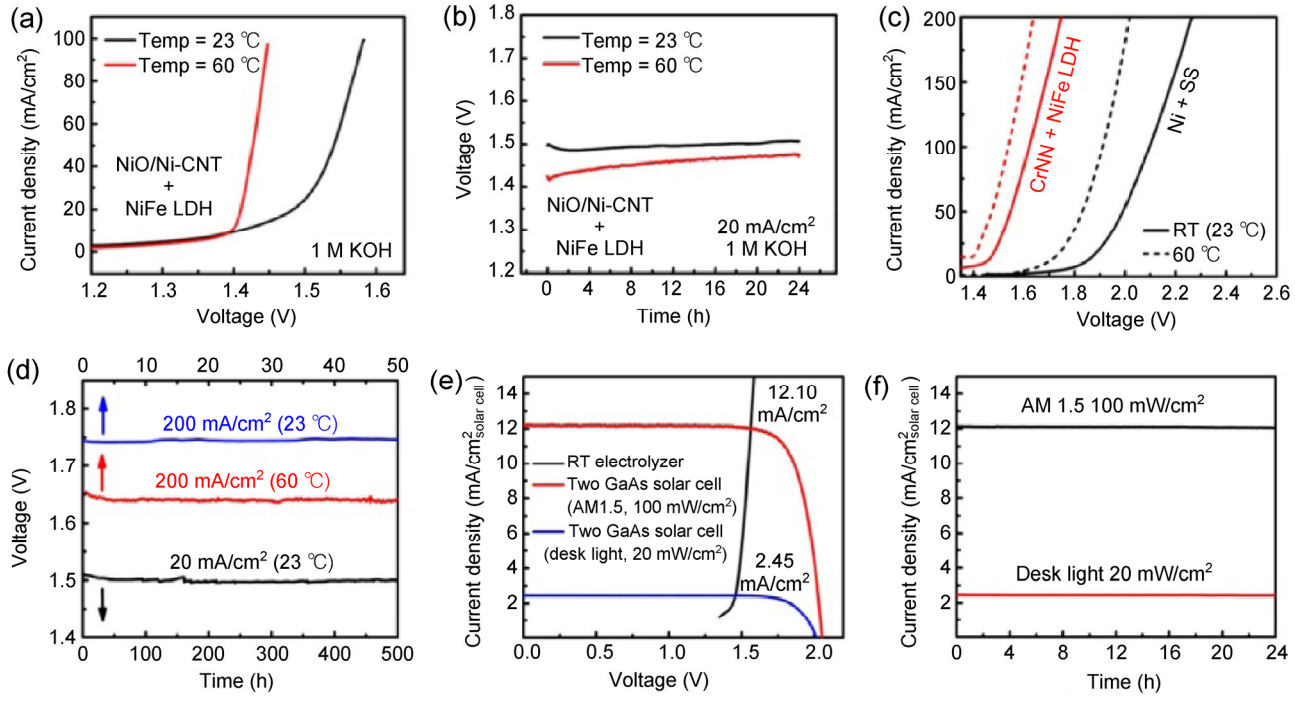

Figure 7 (a) LSV curves of the electrolyzer using NiO/Ni-CNT catalyst as cathode (8 mg/cm^2) and NiFe LDH as anode (8 mg/cm^2) at room temperature (RT, 23 °C) and 60 °C at a scan rate of 1 mV/s with *iR* compensation. (b) *i*–*t* curves of the electrolyzer with NiO/Ni-CNT and NiFe LDH catalysts at a constant current density of 20 mA/cm^2 at 23 and 60 °C. (Reprinted with permission from Ref. [93], © Nature Publishing Group.) (c) LSV curves of the electrolyzer using a CrNN catalyst as cathode (24 mg/cm^2 with 30 wt.% Ni powder) and NiFe LDH as anode (20 mg/cm^2 with 30 wt.% Ni powder) compared to a Ni foil cathode and stainless steel (SS) foil anode at 23 and 60 °C at a scan rate of 1 mV/s. (Not *iR*-compensated, R = ~0.9 Ω for both electrolyzers). (d) *i*–*t* curves of the electrolyzer with CrNN and NiFe LDH catalysts at different constant current densities at RT and 60 °C. (e) Solar cell *i*–*V* curves of two GaAs solar cells in series under simulated sunlight AM 1.5 100 mW/cm^2 and LED desk light 20 mW/cm^2, overlapped with the *i*–*V* curves of the electrolyzer. (f) *i*–*t* curves of solar water splitting driven by the GaAs solar cells under simulated sunlight AM 1.5 100 mW/cm^2 and LED desk light 20 mW/cm^2. (Reprinted with permission from Ref. [94], © Wiley-VCH Verlag GmbH & Co. KGaA, Weinheim 2015.)

electrolyzer has also been reported by other studies. The bifunctional 2-cycle $NiFeO_x$/CFP through Li^+ insertion/extraction could deliver ~10 mA/cm^2 of water splitting current density at a voltage of ~1.51 V for at least 200 h in 1 M KOH (Fig. 3(c)) [84]. The electrolyzer consisting of NiFe LDH/Ni foam electrodes (as both HER and OER catalysts) coupled to a promising perovskite-based solar cell gives a solar-driven water splitting device with ~12.3% efficiency using low-cost materials [83]. Among electrolyzers using non-precious metal materials, the unique combination of a CrNN catalyst for hydrogen evolution and a NiFe LDH catalyst for oxygen evolution offered the best activity and stability, being highly promising for low-cost industrial alkaline electrolysis.

An alternative to alkaline electrolysis is the chloralkali process that replaces alkaline water electrolytes with brine, i.e. NaCl containing water. The chloralkali industry consumes billions of kWh of energy per year in the U.S., accounting for approximately 2% of the total electricity consumption. Lowering the voltage by novel catalysts could significantly save the energy cost by billions of dollars. In the chloralkali process, the cathode undergoes a HER process to produce H_2 and NaOH (caustic soda), while the anode counterpart undergoes chloride oxidation to produce chlorine gas (ClER). The industrial chloralkali process uses nickel metal that occasionally incorporates Pt particles as the HER catalyst and a dimensionally stable anode (RuO_2-based) as the ClER catalyst [95–97], and the chloralkali reactor is usually operated at over 3 V to obtain a fast production of Cl_2. Since HER in brine generates OH^- anion to turn the pH into alkaline condition, most HER catalysts that are developed for

alkaline water electrolysis could work for the chloralkali process. For the relatively mature industry, minimal effort has been undertaken to enhance the electrocatalytic chloralkali process. Nevertheless, several groups have reported using non-precious metal (mainly Ni-based) catalysts to lower the cost of the cathode component. For example, Ni-Fe-C electrodeposits on steel could catalyze H_2 evolution in brine at pH 12 at an elevated temperature of 90 ℃, with an overpotential of only 65 mV [98].

Artificial photosynthesis has attracted much attention in capturing and converting sunlight directly into chemical fuels. Photo-electrochemical water splitting is a promising route of artificial photosynthesis to obtain H_2 at a lower cost, but putting solar absorbers into the electrolyte usually requires a protection layer that prevents the absorbers from corrosion. A catalyst layer on the light absorber is also needed to facilitate H_2 or O_2 generation [99, 100]. Researchers usually utilize Pt as the HER catalyst owing to its fast kinetics and easy handling, but a recent focus has been on finding cheap substitutes for Pt. Our group utilized a thin Ni film as a dual-functional layer that acts as a HER catalyst and protection on top of titanium-coated p-type silicon for the photo-electrochemical water reduction in alkaline electrolytes [100]. The photocathode could afford an onset potential of ~0.3 V vs. RHE in 1 M KOH and similar catalytic activity, but with improved stability in potassium borate buffer solution. As bare metallic nickel is not ideal for hydrogen evolution, researchers have investigated other active candidates for the photo-electrochemical water reduction process. McKone et al. previously evaluated the activity of electrodeposited Ni and Ni-Mo alloy catalysts on crystalline silicon electrodes, and observed similar activity between Ni and Ni-Mo electrocatalysts on Si photocathodes under light irradiation, even though Ni-Mo catalysts have obvious advantages over Ni catalysts in dark (Fig. 8) [101]. Therefore, despite the presence of highly active Ni-based or non-precious metal-based HER catalysts, constructing a high quality thin-film catalyst and catalyst/absorber interface is still a highly challenging but important task to achieve artificial leaves with high efficiency.

Incorporating biosystems into energy-related devices is undergoing rapid development. A typical example is the microbial electrolysis cell (MEC). In an MEC, exoelectrogenic bacteria consume organic matter, producing electrons, protons, and CO_2 on the anode. Electrons and protons subsequently migrate to the cathode and combine with each other to form H_2. An additional voltage of >0.2 V is usually required to drive the reaction. Slightly acidic or neutral media are commonly used as electrolyte to ensure the survival of the bacteria [102, 103]. Some efforts have been invested in replacing Pt-based catalyst on the cathode with non-precious metal catalyst, such as Ni, in the MECs. For instance, Ni powder was discovered to show only slightly lower maximum hydrogen production rate than Pt in an MEC as reported by Selembo et al., and Ni dissolution could be further

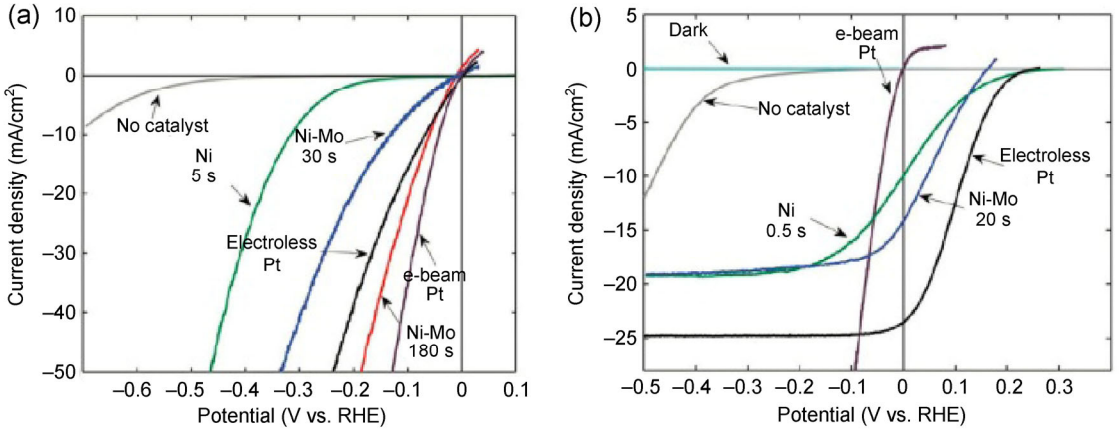

Figure 8 (a) Comparison of the HER activities of various catalysts on p^+-Si microwires. (b) Comparison of the HER activities of various catalysts on p-Si photocathodes under illumination. (Reproduced with permission from Ref. [101], © Royal Society of Chemistry 2011.)

minimized by replacing the medium [104]. The concept and prototype of MEC are still in early stages and thus require further research into finding more efficient bacteria, as well as compatible non-precious metal electrocatalysts with high activity.

6 Conclusions

This review summarizes some of the historically important works on alkaline HER catalysis on Ni surfaces, as well as some recent approaches to improving Ni-based HER catalysts. We also briefly reviewed the applications of HER. Heterogeneous HER catalysis in alkaline media proceeds via two general mechanisms (Volmer-Tafel or Volmer-Heyrovsky mechanisms), and these reactions differ from those in acidic media. Many previous studies have focused on determining the mechanism of HER on Ni surfaces, including measuring the rate-determining step and hydride behavior over HER operation, but it remains controversial and may involve different mechanisms at different potentials and current densities. Nevertheless, researchers have invested much effort into optimizing Ni-based catalysts in various aspects and these catalysts hold great potential in catalyzing HER under alkaline conditions with comparable activity to the most active HER catalysts operating in acid and close to that of Pt-based catalysts (Table 1). Creating nano-sized metallic Ni catalysts can dramatically improve the current increase at higher overpotential owing to larger surface areas but this fails to improve the overpotential at the onset owing to the same chemical nature. Incorporating additional elements into metallic Ni to form alloys provides more opportunities to fine-tune the adsorption properties of the catalyst surface and thereby, greatly enhances the catalytic activity. Specifically, Ni-Mo-based alloys stand out among all Ni-based alloy catalysts and exhibit superior activity towards HER catalysis in alkaline condition, but the underlying mechanism responsible for the improvement remains elusive. Nickel-based oxide/hydroxide, generally considered as HER-inactive materials, becomes potentially active materials after fine-tuning their surface electronic property (e.g. by lithium ion insertion/extraction cycles).

Meanwhile, nickel sulfide/phosphide exhibited promising activity towards HER in acidic media, but was chemically unstable under alkaline media. The discovery of hetero-structure-based catalyst offers new opportunities in forming novel interfaces for HER catalysis. By tailoring the oxide/hydroxide-metal interfaces, a much improved HER activity was obtained

Table 1 Summary of the HER catalytic activity of representative catalysts

Catalyst	Loading (mg/cm^2)	Electrolyte	Overpotential (mV)	Current density (mA/cm^2)	Reference
NiO/Ni-CNT	0.28	1 M KOH	80	10	[93]
NiO/Ni-CNT	8	1 M KOH	95	100	[93]
Ni@NiO-Cr_2O_3	24	1 M KOH	115 (no *iR* compensation)	100	[94]
Ni-Mo nanopowder	1.0	2 M KOH	70	20	[81]
Ni-Mo nanopowder	3.0	0.5 M H_2SO_4	80	20	[81]
Ni-Mo nanopowder	13.4	2 M KOH	100	130	[81]
2-Cylce $NiFeO_x$	1.6	1 M KOH	~220	100	[84]
CoP on Ti	0.2	0.5 M H_2SO_4	~85	20	[33]
Ni_2P	1	0.5 M H_2SO_4	130	20	[25]
$CoSe_2$	2.8	0.5 M H_2SO_4	180	100	[32]
MoS_2/RGO	0.28	0.5 M H_2SO_4	150	10	[22]
Ni-Mo-N nanosheet	0.25	0.1 M $HClO_4$	200	3.5	[85]
Pt/C	0.28	0.5 M H_2SO_4	~50	20	[22]
Pt/C	8	1 M KOH	~50	100	[93]

when compared to bare metal surfaces, owing to the different adsorption behaviors of H, H_2O, and OH^-. Maximizing the interfaces by synthetic approaches could produce a highly active HER catalyst in alkaline condition based on low-cost NiO-Ni heterostructures. Further incorporation of chemically stable Cr_2O_3 on NiO-Ni active sites could lead to a promising non-precious metal-based HER catalyst with both high activity and stability in basic conditions. Finally, selected applications of the Ni-based alkaline HER catalysts were discussed, including water splitting, the chloralkali process, photo-electrochemical water splitting, and microbial electrolysis cell. The present and future developments of highly active Ni-based catalysts could greatly lower the cost of hydrogen economy and boost the utilization of clean and renewable energy.

Acknowledgements

This work was supported by a Grant from Stanford GCEP, a Steinhart/Reed Award from the Stanford Precourt Institute for Energy, the Global Networking Talent 3.0 plan (NTUST 104DI005) from "the Ministry of Education of Taiwan", China and by the U.S. Department of Energy, Office of Basic Energy Sciences, Division of Materials Sciences and Engineering under Award # DOE DE-SC0008684 (for carbon nanomaterials synthesis and characterization with advanced electrical properties).

References

[1] Cook, T. R.; Dogutan, D. K.; Reece, S. Y.; Surendranath, Y.; Teets, T. S.; Nocera, D. G. Solar energy supply and storage for the legacy and nonlegacy worlds. *Chem. Rev.* **2010**, *110*, 6474–6502.

[2] Gray, H. B. Powering the planet with solar fuel. *Nat. Chem.* **2009**, *1*, 7.

[3] Kudo, A.; Miseki, Y. Heterogeneous photocatalyst materials for water splitting. *Chem. Soc. Rev.* **2009**, *38*, 253–278.

[4] Lewis, N. S.; Nocera, D. G. Powering the planet: Chemical challenges in solar energy utilization. *Proc. Natl. Acad. Sci. USA* **2006**, *103*, 15729–15735.

[5] Liang, Y. Y.; Li, Y. G.; Wang, H. L.; Dai, H. J. Strongly coupled inorganic/nanocarbon hybrid materials for advanced electrocatalysis. *J. Am. Chem. Soc.* **2013**, *135*, 2013–2036.

[6] Walter, M. G.; Warren, E. L.; McKone, J. R.; Boettcher, S. W.; Mi, Q. X.; Santori, E. A.; Lewis, N. S. Solar water splitting cells. *Chem. Rev.* **2010**, *110*, 6446–6473.

[7] Wang, H. L.; Dai, H. J. Strongly coupled inorganic–nano-carbon hybrid materials for energy storage. *Chem. Soc. Rev.* **2013**, *42*, 3088–3113.

[8] Crabtree, G. W.; Dresselhaus, M. S.; Buchanan, M. V. The hydrogen economy. *Physics Today* **2004**, *57*, 39–44.

[9] Dresselhaus, M. S.; Thomas, I. L. Alternative energy technologies. *Nature* **2001**, *414*, 332–337.

[10] Häussinger, P.; Lohmüller, R.; Watson, A. M. Hydrogen. In *Ullmann's Encyclopedia of Industrial Chemistry*; Wiley-VCH: Weinheim, Germany, 2000.

[11] Carmo, M.; Fritz, D. L.; Mergel, J.; Stolten, D. A comprehensive review on pem water electrolysis. *Int. J. Hydrogen Energy* **2013**, *38*, 4901–4934.

[12] Gong, M.; Dai, H. J. A mini review of nife-based materials as highly active oxygen evolution reaction electrocatalysts. *Nano Res.* **2015**, *8*, 23–39.

[13] Holladay, J. D.; Hu, J.; King, D. L.; Wang, Y. An overview of hydrogen production technologies. *Catal. Today* **2009**, *139*, 244–260.

[14] Zeng, K.; Zhang, D. K. Recent progress in alkaline water electrolysis for hydrogen production and applications. *Prog. Energy Combust. Sci.* **2010**, *36*, 307–326.

[15] Lasia, A. Hydrogen evolution reaction. In *Handbook of Fuel Cells*; John Wiley & Sons: New York, 2010.

[16] Danilovic, N.; Subbaraman, R.; Strmcnik, D.; Stamenkovic, V. R.; Markovic, N. M. Electrocatalysis of the her in acid and alkaline media. *J. Serb. Chem. Soc.* **2013**, *78*, 2007–2015.

[17] Nørskov, J. K.; Bligaard, T.; Logadottir, A.; Kitchin, J. R.; Chen, J. G.; Pandelov, S.; Stimming, U. Trends in the exchange current for hydrogen evolution. *J. Electrochem. Soc.* **2005**, *152*, J23–J26.

[18] Greeley, J.; Jaramillo, T. F.; Bonde, J.; Chorkendorff, I.; Nørskov, J. K. Computational high-throughput screening of electrocatalytic materials for hydrogen evolution. *Nat. Mater.* **2006**, *5*, 909–913.

[19] Hinnemann, B.; Moses, P. G.; Bonde, J.; Jørgensen, K. P.; Nielsen, J. H.; Horch, S.; Chorkendorff, I.; Nørskov, J. K. Biomimetic hydrogen evolution: MoS_2 nanoparticles as catalyst for hydrogen evolution. *J. Am. Chem. Soc.* **2005**, *127*, 5308–5309.

[20] Jaramillo, T. F.; Jørgensen, K. P.; Bonde, J.; Nielsen, J. H.; Horch, S.; Chorkendorff, I. Identification of active edge sites for electrochemical H_2 evolution from MoS_2 nanocatalysts. *Science* **2007**, *317*, 100–102.

[21] Bonde, J.; Moses, P. G.; Jaramillo, T. F.; Nørskov, J. K.; Chorkendorff, I. Hydrogen evolution on nano-particulate

transition metal sulfides. *Faraday Discuss.* **2009**, *140*, 219–231.

[22] Li, Y. G.; Wang, H. L.; Xie, L. M.; Liang, Y. Y.; Hong, G. S.; Dai, H. J. MoS_2 nanoparticles grown on graphene: An advanced catalyst for the hydrogen evolution reaction. *J. Am. Chem. Soc.* **2011**, *133*, 7296–7299.

[23] Choi, C. L.; Feng, J.; Li, Y. G.; Wu, J.; Zak, A.; Tenne, R.; Dai, H. J. WS_2 nanoflakes from nanotubes for electrocatalysis. *Nano Res.* **2013**, *6*, 921–928.

[24] Kong, D. S.; Cha, J. J.; Wang, H. T.; Lee, H. R.; Cui, Y. First-row transition metal dichalcogenide catalysts for hydrogen evolution reaction. *Energy Environ. Sci.* **2013**, *6*, 3553–3558.

[25] Popczun, E. J.; McKone, J. R.; Read, C. G.; Biacchi, A. J.; Wiltrout, A. M.; Lewis, N. S.; Schaak, R. E. Nanostructured nickel phosphide as an electrocatalyst for the hydrogen evolution reaction. *J. Am. Chem. Soc.* **2013**, *135*, 9267–9270.

[26] Voiry, D.; Yamaguchi, H.; Li, J. W.; Silva, R.; Alves, D. C. B.; Fujita, T.; Chen, M. W.; Asefa, T.; Shenoy, V. B.; Eda, G. et al. Enhanced catalytic activity in strained chemically exfoliated WS_2 nanosheets for hydrogen evolution. *Nat. Mater.* **2013**, *12*, 850–855.

[27] Cheng, L.; Huang, W. J.; Gong, Q. F.; Liu, C. H.; Liu, Z.; Li, Y. G.; Dai, H. J. Ultrathin WS_2 nanoflakes as a high-performance electrocatalyst for the hydrogen evolution reaction. *Angew. Chem., Int. Ed.* **2014**, *53*, 7860–7863.

[28] Faber, M. S.; Dziedzic, R.; Lukowski, M. A.; Kaiser, N. S.; Ding, Q.; Jin, S. High-performance electrocatalysis using metallic cobalt pyrite (CoS_2) micro- and nanostructures. *J. Am. Chem. Soc.* **2014**, *136*, 10053–10061.

[29] Faber, M. S.; Lukowski, M. A.; Ding, Q.; Kaiser, N. S.; Jin, S. Earth-abundant metal pyrites (FeS_2, CoS_2, NiS_2, and their alloys) for highly efficient hydrogen evolution and polysulfide reduction electrocatalysis. *J. Phys. Chem. C* **2014**, *118*, 21347–21356.

[30] Gao, M.-R.; Cao, X.; Gao, Q.; Xu, Y.-F.; Zheng, Y.-R.; Jiang, J.; Yu, S.-H. Nitrogen-doped graphene supported $CoSe_2$ nanobelt composite catalyst for efficient water oxidation. *ACS Nano* **2014**, *8*, 3970–3978.

[31] Jiang, P.; Liu, Q.; Liang, Y. H.; Tian, J. Q.; Asiri, A. M.; Sun, X. P. A cost-effective 3D hydrogen evolution cathode with high catalytic activity: FeP nanowire array as the active phase. *Angew. Chem., Int. Ed.* **2014**, *53*, 12855–12859.

[32] Kong, D. S.; Wang, H. T.; Lu, Z. Y.; Cui, Y. $CoSe_2$ nanoparticles grown on carbon fiber paper: An efficient and stable electrocatalyst for hydrogen evolution reaction. *J. Am. Chem. Soc.* **2014**, *136*, 4897–4900.

[33] Popczun, E. J.; Read, C. G.; Roske, C. W.; Lewis, N. S.; Schaak, R. E. Highly active electrocatalysis of the hydrogen evolution reaction by cobalt phosphide nanoparticles. *Angew. Chem.* **2014**, *126*, 5531–5534.

[34] Wang, H. T.; Tsai, C.; Kong, D. S.; Chan, K. R.; Abild-Pedersen, F.; Nørskov, J. K.; Cui, Y. Transition-metal doped edge sites in vertically aligned MoS_2 catalysts for enhanced hydrogen evolution. *Nano Res.* **2015**, *8*, 566–575.

[35] Zhang, Y. J.; Gong, Q. F.; Li, L.; Yang, H. C.; Li, Y. G.; Wang, Q. B. $MoSe_2$ porous microspheres comprising monolayer flakes with high electrocatalytic activity. *Nano Res.* **2015**, *8*, 1108–1115.

[36] Wang, D.-Y.; Gong, M.; Chou, H.-L.; Pan, C.-J.; Chen, H.-A.; Wu, Y. P.; Lin, M.-C.; Guan, M. Y.; Yang, J.; Chen, C.-W. et al. Highly active and stable hybrid catalyst of cobalt-doped FeS_2 nanosheets–carbon nanotubes for hydrogen evolution reaction. *J. Am. Chem. Soc.* **2015**, *137*, 1587–1592.

[37] Merrill, M. D.; Dougherty, R. C. Metal oxide catalysts for the evolution of O_2 from H_2O. *J. Phys. Chem. C* **2008**, *112*, 3655–3666.

[38] Jiao, F.; Frei, H. Nanostructured cobalt and manganese oxide clusters as efficient water oxidation catalysts. *Energy Environ. Sci.* **2010**, *3*, 1018–1027.

[39] Bediako, D. K.; Lassalle-Kaiser, B.; Surendranath, Y.; Yano, J.; Yachandra, V. K.; Nocera, D. G. Structure–activity correlations in a nickel-borate oxygen evolution catalyst. *J. Am. Chem. Soc.* **2012**, *134*, 6801–6809.

[40] Trotochaud, L.; Ranney, J. K.; Williams, K. N.; Boettcher, S. W. Solution-cast metal oxide thin film electrocatalysts for oxygen evolution. *J. Am. Chem. Soc.* **2012**, *134*, 17253–17261.

[41] Gong, M.; Li, Y. G.; Wang, H. L.; Liang, Y. Y.; Wu, J. Z.; Zhou, J. G.; Wang, J.; Regier, T.; Wei, F.; Dai, H. J. An advanced Ni–Fe layered double hydroxide electrocatalyst for water oxidation. *J. Am. Chem. Soc.* **2013**, *135*, 8452–8455.

[42] Louie, M. W.; Bell, A. T. An investigation of thin-film Ni–Fe oxide catalysts for the electrochemical evolution of oxygen. *J. Am. Chem. Soc.* **2013**, *135*, 12329–12337.

[43] McCrory, C. C. L.; Jung, S.; Peters, J. C.; Jaramillo, T. F. Benchmarking heterogeneous electrocatalysts for the oxygen evolution reaction. *J. Am. Chem. Soc.* **2013**, *135*, 16977–16987.

[44] Tüysüz, H.; Hwang, Y. J.; Khan, S. B.; Asiri, A. M.; Yang, P. D. Mesoporous Co_3O_4 as an electrocatalyst for water oxidation. *Nano Res.* **2013**, *6*, 47–54.

[45] Lu, Z. Y.; Wang, H. T.; Kong, D.; Yan, K.; Hsu, P.-C.; Zheng, G. Y.; Yao, H. B.; Liang, Z.; Sun, X. M.; Cui, Y. Electrochemical tuning of layered lithium transition metal oxides for improvement of oxygen evolution reaction. *Nat. Commun.* **2014**, *5*, 4345.

[46] Song, F.; Hu, X. L. Exfoliation of layered double hydroxides for enhanced oxygen evolution catalysis. *Nat. Commun.* **2014**, *5*, 4477.

[47] Davis, J. R. *Nickel, Cobalt, and Their Alloys*; ASM international: Materials Park, OH, 2000.

[48] Stoney, G. G. The tension of metallic films deposited by electrolysis. *Proc. Roy. Soc. Lond. A* **1909**, *82*, 172–175.

[49] Fournier, J.; Brossard, L.; Tilquin, J. Y.; Coté, R.; Dodelet, J. P.; Guay, D.; Ménard, H. Hydrogen evolution reaction in alkaline solution: Catalytic influence of pt supported on graphite vs. Pt inclusions in graphite. *J. Electrochem. Soc.* **1996**, *143*, 919–926.

[50] Sheng, W. C.; Gasteiger, H. A.; Shao-Horn, Y. Hydrogen oxidation and evolution reaction kinetics on platinum: Acid vs. alkaline electrolytes. *J. Electrochem. Soc.* **2010**, *157*, B1529–B1536.

[51] Devanathan, M. A. V.; Selvaratnam, M. Mechanism of the hydrogen-evolution reaction on nickel in alkaline solutions by the determination of the degree of coverage. *Trans. Faraday Soc.* **1960**, *56*, 1820–1831.

[52] Miles, M.; Kissel, G.; Lu, P. W. T.; Srinivasan, S. Effect of temperature on electrode kinetic parameters for hydrogen and oxygen evolution reactions on nickel electrodes in alkaline solutions. *J. Electrochem. Soc.* **1976**, *123*, 332–336.

[53] Krstajić, N.; Popović, M.; Grgur, B.; Vojnović, M.; Šepa, D. On the kinetics of the hydrogen evolution reaction on nickel in alkaline solution: Part I. The mechanism. *J. Electroanal. Chem.* **2001**, *512*, 16–26.

[54] Diard, J.-P.; LeGorrec, B.; Maximovitch, S. Etude de l'activation du degagement d'hydrogene sur electrode d'oxyde de nickel par spectroscopie d'impedance. *Electrochim. Acta* **1990**, *35*, 1099–1108.

[55] Kreysa, G.; Hakansson, B.; Ekdunge, P. Kinetic and thermodynamic analysis of hydrogen evolution at nickel electrodes. *Electrochim. Acta* **1988**, *33*, 1351–1357.

[56] LeRoy, R. L.; Janjua, M. B. I.; Renaud, R.; Leuenberger, U. Analysis of time-variation effects in water electrolyzers. *J. Electrochem. Soc.* **1979**, *126*, 1674–1682.

[57] Soares, D. M.; Teschke, O.; Torriani, I. Hydride effect on the kinetics of the hydrogen evolution reaction on nickel cathodes in alkaline media. *J. Electrochem. Soc.* **1992**, *139*, 98–105.

[58] Bernardini, M.; Comisso, N.; Davolio, G.; Mengoli, G. Formation of nickel hydrides by hydrogen evolution in alkaline media. *J. Electroanal. Chem.* **1998**, *442*, 125–135.

[59] Weininger, J. L.; Breiter, M. W. Hydrogen evolution and surface oxidation of nickel electrodes in alkaline solution. *J. Electrochem. Soc.* **1964**, *111*, 707–712.

[60] Raveendran, P.; Fu, J.; Wallen, S. L. Completely "green" synthesis and stabilization of metal nanoparticles. *J. Am. Chem. Soc.* **2003**, *125*, 13940–13941.

[61] Grzelczak, M.; Pérez-Juste, J.; Mulvaney, P.; Liz-Marzán, L. M. Shape control in gold nanoparticle synthesis. *Chem. Soc. Rev.* **2008**, *37*, 1783–1791.

[62] Ghosh Chaudhuri, R.; Paria, S. Core/shell nanoparticles: Classes, properties, synthesis mechanisms, characterization, and applications. *Chem. Rev.* **2012**, *112*, 2373–2433.

[63] Lin, Y.-Y.; Wang, D.-Y.; Yen, H.-C.; Chen, H.-L.; Chen, C.-C.; Chen, C.-M.; Tang, C.-Y.; Chen, C.-W. Extended red light harvesting in a poly(3-hexylthiophene)/iron disulfide nanocrystal hybrid solar cell. *Nanotechnology* **2009**, *20*, 405207.

[64] Wang, D. Y.; Jiang, Y. T.; Lin, C. C.; Li, S. S.; Wang, Y. T.; Chen, C. C.; Chen, C. W. Solution-processable pyrite FeS_2 nanocrystals for the fabrication of heterojunction photodiodes with visible to nir photodetection. *Adv. Mater.* **2012**, *24*, 3415–3420.

[65] Wang, Y. C.; Wang, D. Y.; Jiang, Y. T.; Chen, H. A.; Chen, C. C.; Ho, K. C.; Chou, H. L.; Chen, C. W. FeS_2 nanocrystal ink as a catalytic electrode for dye-sensitized solar cells. *Angew. Chem., Int. Ed.* **2013**, *52*, 6694–6698.

[66] Chen, D.-H.; Wu, S.-H. Synthesis of nickel nanoparticles in water-in-oil microemulsions. *Chem. Mater.* **2000**, *12*, 1354–1360.

[67] Wu, S.-H.; Chen, D.-H. Synthesis and characterization of nickel nanoparticles by hydrazine reduction in ethylene glycol. *J. Colloid Interf. Sci.* **2003**, *259*, 282–286.

[68] Sahiner, N.; Ozay, H.; Ozay, O.; Aktas, N. New catalytic route: Hydrogels as templates and reactors for *in situ* Ni nanoparticle synthesis and usage in the reduction of 2- and 4-nitrophenols. *Appl. Catal. A: Gen.* **2010**, *385*, 201–207.

[69] Zhang, H. G.; Yu, X. D.; Braun, P. V. Three-dimensional bicontinuous ultrafast-charge and -discharge bulk battery electrodes. *Nat. Nanotechnol.* **2011**, *6*, 277–281.

[70] Gong, M.; Li, Y. G.; Zhang, H. B.; Zhang, B.; Zhou, W.; Feng, J.; Wang, H. L.; Liang, Y. Y.; Fan, Z. J.; Liu, J. et al. Ultrafast high-capacity NiZn battery with NiAlCo-layered double hydroxide. *Energy Environ Sci* **2014**, *7*, 2025–2032.

[71] Zhou, H. H.; Peng, C. Y.; Jiao, S. Q.; Zeng, W.; Chen, J. H.; Kuang, Y. F. Electrodeposition of nanoscaled nickel in a reverse microemulsion. *Electrochem. Commun.* **2006**, *8*, 1142–1146.

[72] Hang, T.; Hu, A. M.; Ling, H. Q.; Li, M.; Mao, D. L. Super-hydrophobic nickel films with micro-nano hierarchical structure prepared by electrodeposition. *Appl. Surf. Sci.* **2010**, *256*, 2400–2404.

[73] Ahn, S. H.; Hwang, S. J.; Yoo, S. J.; Choi, I.; Kim, H.-J.; Jang, J. H.; Nam, S. W.; Lim, T.-H.; Lim, T.; Kim, S.-K. et al. Electrodeposited Ni dendrites with high activity and durability for hydrogen evolution reaction in alkaline water electrolysis. *J. Mater. Chem.* **2012**, *22*, 15153–15159.

[74] McArthur, M. A.; Jorge, L.; Coulombe, S.; Omanovic, S. Synthesis and characterization of 3D Ni nanoparticle/carbon nanotube cathodes for hydrogen evolution in alkaline electrolyte. *J. Power Sources* **2014**, *266*, 365–373.

[75] Brown, D. E.; Mahmood, M. N.; Man, M. C. M.; Turner, A. K. Preparation and characterization of low overvoltage transition metal alloy electrocatalysts for hydrogen evolution in alkaline solutions. *Electrochim. Acta* **1984**, *29*, 1551–1556.

[76] Raj, I. A.; Vasu, K. I. Transition metal-based hydrogen electrodes in alkaline solution—Electrocatalysis on nickel based binary alloy coatings. *J. Appl. Electrochem.* **1990**, *20*, 32–38.

[77] Raj, I. A.; Vasu, K. I. Transition metal-based cathodes for hydrogen evolution in alkaline solution: Electrocatalysis on nickel-based ternary electrolytic codeposits. *J. Appl. Electrochem.* **1992**, *22*, 471–477.

[78] Angelo, A. C. D.; Lasia, A. Surface effects in the hydrogen evolution reaction on Ni–Zn alloy electrodes in alkaline solutions. *J. Electrochem. Soc.* **1995**, *142*, 3313–3319.

[79] Lupi, C.; Dell'Era, A.; Pasquali, M. Nickel–cobalt electrodeposited alloys for hydrogen evolution in alkaline media. *Int. J. Hydrogen Energy* **2009**, *34*, 2101–2106.

[80] Dong, H. X.; Lei, T.; He, Y. H.; Xu, N. P.; Huang, B. Y.; Liu, C. T. Electrochemical performance of porous Ni_3Al electrodes for hydrogen evolution reaction. *Int. J. Hydrogen Energy* **2011**, *36*, 12112–12120.

[81] McKone, J. R.; Sadtler, B. F.; Werlang, C. A.; Lewis, N. S.; Gray, H. B. Ni–Mo nanopowders for efficient electrochemical hydrogen evolution. *ACS Catal.* **2013**, *3*, 166–169.

[82] Campbell, J. A.; Whiteker, R. A. A periodic table based on potential–pH diagrams. *J. Chem. Educ.* **1969**, *46*, 90.

[83] Luo, J.; Im, J.-H.; Mayer, M. T.; Schreier, M.; Nazeeruddin, M. K.; Park, N.-G.; Tilley, S. D.; Fan, H. J.; Grätzel, M. Water photolysis at 12.3% efficiency via perovskite photovoltaics and earth-abundant catalysts. *Science* **2014**, *345*, 1593–1596.

[84] Wang, H. T.; Lee, H.-W.; Deng, Y.; Lu, Z. Y.; Hsu, P.-C.; Liu, Y. Y.; Lin, D. C.; Cui, Y. Bifunctional non-noble metal oxide nanoparticle electrocatalysts through lithium-induced conversion for overall water splitting. *Nat. Commun.* **2015**, *6*, 7261.

[85] Chen, W. F.; Sasaki, K.; Ma, C.; Frenkel, A. I.; Marinkovic, N.; Muckerman, J. T.; Zhu, Y. M.; Adzic, R. R. Hydrogen-evolution catalysts based on non-noble metal nickel–molybdenum nitride nanosheets. *Angew. Chem., Int. Ed.* **2012**, *51*, 6131–6135.

[86] Han, Q.; Liu, K. R.; Chen, J. S.; Wei, X. J. A study on the electrodeposited Ni–S alloys as hydrogen evolution reaction cathodes. *Int. J. Hydrogen Energy* **2003**, *28*, 1207–1212.

[87] Paseka, I. Evolution of hydrogen and its sorption on remarkable active amorphous smooth Ni–P(x) electrodes. *Electrochim. Acta* **1995**, *40*, 1633–1640.

[88] Burchardt, T. Hydrogen evolution on NiP_x alloys: The influence of sorbed hydrogen. *Int. J. Hydrogen Energy* **2001**, *26*, 1193–1198.

[89] Feng, L. G.; Vrubel, H.; Bensimon, M.; Hu, X. L. Easily-prepared dinickel phosphide (Ni_2P) nanoparticles as an efficient and robust electrocatalyst for hydrogen evolution. *Phys. Chem. Chem. Phys.* **2014**, *16*, 5917–5921.

[90] Jin, Z. Y.; Li, P. P.; Huang, X.; Zeng, G. F.; Jin, Y.; Zheng, B. Z.; Xiao, D. Three-dimensional amorphous tungsten-doped nickel phosphide microsphere as an efficient electrocatalyst for hydrogen evolution. *J. Mater. Chem. A* **2014**, *2*, 18593–18599.

[91] Subbaraman, R.; Tripkovic, D.; Strmcnik, D.; Chang, K.-C.; Uchimura, M.; Paulikas, A. P.; Stamenkovic, V.; Markovic, N. M. Enhancing hydrogen evolution activity in water splitting by tailoring Li^+–$Ni(OH)_2$–Pt interfaces. *Science* **2011**, *334*, 1256–1260.

[92] Danilovic, N.; Subbaraman, R.; Strmcnik, D.; Chang, K. C.; Paulikas, A. P.; Stamenkovic, V. R.; Markovic, N. M. Enhancing the alkaline hydrogen evolution reaction activity through the bifunctionality of $Ni(OH)_2$/metal catalysts. *Angew. Chem.* **2012**, *124*, 12663–12666.

[93] Gong, M.; Zhou, W.; Tsai, M.-C.; Zhou, J. G.; Guan, M. Y.; Lin, M.-C.; Zhang, B.; Hu, Y. F.; Wang, D.-Y.; Yang, J. et al. Nanoscale nickel oxide/nickel heterostructures for active hydrogen evolution electrocatalysis. *Nat. Commun.* **2014**, *5*, 4695.

[94] Gong, M.; Zhou, W.; Kenney, M. J.; Kapusta, R.; Cowley, S.; Wu, Y. P.; Lu, B. G.; Lin, M. C.; Wang, D. Y.; Yang, J. et al. Blending Cr_2O_3 into a NiO–Ni electrocatalyst for sustained water splitting. *Angew. Chem.* **2015**, *127*, 12157–12161.

[95] Duby, P. The history of progress in dimensionally stable anodes. *JOM* **1993**, *45*, 41–43.

[96] Yoshida, N.; Morimoto, T. A new low hydrogen overvoltage cathode for chlor–alkali electrolysis cell. *Electrochim. Acta* **1994**, *39*, 1733–1737.

[97] Pilla, A. S.; Cobo, E. O.; Duarte, M. M. E.; Salinas, D. R. Evaluation of anode deactivation in chlor–alkali cells. *J. Appl. Electrochem.* **1997**, *27*, 1283–1289.

[98] Jiang, N.; Meng, H.-M.; Song, L.-J.; Yu, H.-Y. Study on Ni–Fe–C cathode for hydrogen evolution from seawater electrolysis. *Int. J. Hydrogen Energy* **2010**, *35*, 8056–8062.

[99] Kenney, M. J.; Gong, M.; Li, Y.; Wu, J. Z.; Feng, J.; Lanza, M.; Dai, H. High-performance silicon photoanodes passivated with ultrathin nickel films for water oxidation. *Science* **2013**, *342*, 836–840.

[100] Feng, J.; Gong, M.; Kenney, M. J.; Wu, J. Z.; Zhang, B.; Li, Y. G.; Dai, H. J. Nickel-coated silicon photocathode for water splitting in alkaline electrolytes. *Nano Res.* **2015**, *8*, 1577–1583.

[101] McKone, J. R.; Warren, E. L.; Bierman, M. J.; Boettcher, S. W.; Brunschwig, B. S.; Lewis, N. S.; Gray, H. B. Evaluation of Pt, Ni, and Ni–Mo electrocatalysts for hydrogen evolution on crystalline Si electrodes. *Energy Environ. Sci.* **2011**, *4*, 3573–3583.

[102] Rozendal, R. A.; Hamelers, H. V. M.; Euverink, G. J. W.; Metz, S. J.; Buisman, C. J. N. Principle and perspectives of hydrogen production through biocatalyzed electrolysis. *Int. J. Hydrogen Energy* **2006**, *31*, 1632–1640.

[103] Logan, B. E.; Call, D.; Cheng, S. A.; Hamelers, H. V. M.; Sleutels, T. H. J. A.; Jeremiasse, A. W.; Rozendal, R. A. Microbial electrolysis cells for high yield hydrogen gas production from organic matter. *Environ. Sci. Technol.* **2008**, *42*, 8630–8640.

[104] Selembo, P. A.; Merrill, M. D.; Logan, B. E. Hydrogen production with nickel powder cathode catalysts in microbial electrolysis cells. *Int. J. Hydrogen Energy* **2010**, *35*, 428–437.